



XA0300605

Background Material to Pierre Sollogoub's Presentations

**ANALYSIS OF CONFINEMENT
EFFECTS FOR IN-WATER SEISMIC
TESTS ON PWR FUEL ASSEMBLIES**

Daniel Broc, CEA Saclay, France

Jean-Claude Queval, CEA Saclay, France

J. Rigaudeau, Framatome ANP Nuclear Fuel, France

E. Viallet, EDF/SEPTEN, France

ANALYSIS OF CONFINEMENT EFFECTS FOR IN-WATER SEISMIC TESTS ON PWR FUEL ASSEMBLIES

Daniel BROC, Jean-Claude QUEVAL
CEA Saclay

J. RIGAUDEAU
Framatome ANP Nuclear Fuel

E. VIALLET
EDF/SEPTEN

ABSTRACT

In the framework of a comprehensive program on the seismic behaviour of the PWR reactor cores, tests have been performed on a row of six PWR fuel assemblies, with two confinement configurations in water. Global fluid motion along the row is not allowed in the "full confinement configuration", and is allowed in the "lateral confinement configuration". The seismic test results show that the impact forces at assembly grid levels are significantly smaller with the full confinement. This is due to damping, which is found to be larger in this configuration where the average fluid velocity inside the assembly (around the rods) is itself larger. We present analyses of these phenomena from a theoretical and experimental standpoint. This involves both fluid models and structural models of the assembly row.

1 Introduction: PWR seismic studies

The core of a PWR reactor consists of vertical fuel assemblies arranged in a square pitch array (157 assemblies in a 900 MWe reactor). A fuel assembly comprises the fuel rods containing the fissile material, arranged in a square array, and a support "skeleton". The rods are restrained and evenly spaced by grids, themselves regularly spaced and welded on the guide thimbles. The latter, connected to the top and bottom nozzles, ensure mechanical continuity and allow control rod insertion. The fuel assemblies are tall and flexible structures, restrained only at their ends by the upper and lower core plates. The core lateral displacements under seismic loads produce assembly lateral deformations, and impacts between assemblies or with the core baffles at the grid locations. The modeling of the PWR core seismic behaviour comprises two aspects: the modeling of the assemblies, and the modeling of the overall behaviour of the core, with the interactions between assemblies (Figures 1 and 2).

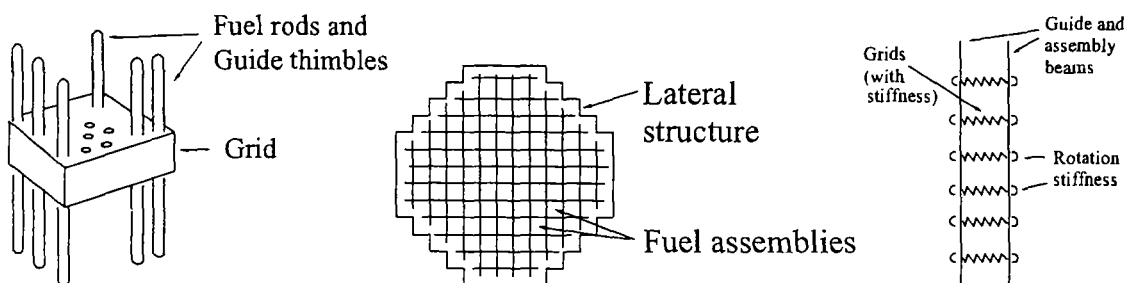


Figure 1: Fuel assembly, reactor core, and two-beam model

Assembly models: Dynamic behaviour models are developed for the assemblies: one- or two-beam models, linear or nonlinear models. Assembly dynamic characterization is performed by means of snap back tests, without impacts, or with impacts on grids, and sine sweep tests. Tests with impacts give characteristics which are used in the global core models.

Global core models: Overall behaviour models usually consider the central row of the core, i.e. a single row of assemblies, loaded in its own direction, with row lateral confinement, i.e. full confinement with the baffles at row ends. Impacts between the assemblies are allowed for by means of springs with gaps. Fluid structure interaction is taken into account with an added mass at assembly, and a coupling term with the core baffles to represent the overall driving of the fluid in the seismic motion; coupling between assemblies is negligible with the confinement hypothesis (see Rigaudau [1] and below). Large damping from the axial coolant is also included, determined from in loop tests. Such damping screens that resulting from drag forces in stagnant water, yet the latter should be considered for the interpretations of seismic tests precisely performed in stagnant water.

Assembly models (embedded at the top and the bottom)

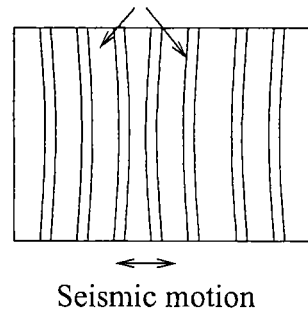
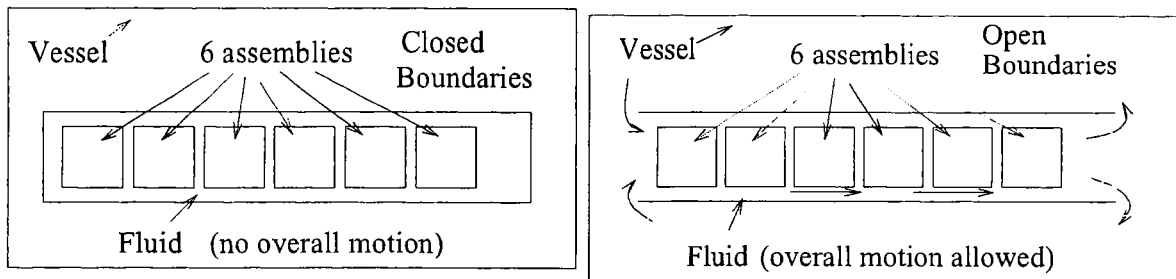


Figure 2: Row model

2 Results of seismic tests

Seismic tests have been recently performed in the framework of a comprehensive program on the seismic behaviour of the PWR cores (Queval [2]). Assembly characterization tests and seismic tests on a six-assembly row have been performed in three configurations: in air, in stagnant water with lateral confinement, and in water with full confinement. Overall fluid motion along the row is not allowed in the "full confinement configuration", and is allowed in the "lateral confinement configuration" with open boundaries at row ends (Figure 3). The impact forces at the grid levels are lower in water than in air, and lower for the full confinement configuration than for the lateral confinement one. In order to explain these results, we have built a fluid structure interaction model for the assembly row, with coupling terms between the assemblies and with the baffles for the inertial effects, and dissipative effects due to the fluid.



FULL CONFINEMENT CONFIGURATION LATERAL CONFINEMENT CONFIGURATION

Figure 3: Confinement configurations

3 Assembly row model

In the present paper, the interpretation of the tests mainly focuses on the fluid structure interaction phenomena. Therefore, the assembly model is a single DOF (degree of freedom) oscillator, presented in the next section (§ 3.1). The in-air row model is built with the assembly characteristics, including impact (§ 3.2), the in-water model from the analysis of the fluid (§ 3.3 to § 3.6).

3.1 Single DOF assembly model in air

The characteristics of the single DOF model for the assembly are determined in the following way. The mass of the oscillator is the mass of a span between grids, i.e. $m = 100$ kg. The stiffness of the oscillator is chosen in order to obtain a frequency close to the first natural frequency of the assembly ($f_{air} = 2.5$ Hz and $\omega_{air} \simeq 16$ Hz). So, the oscillator stiffness is $k = 25\,000$ N/m ($\omega^2 = k/m$). The motion equation of the oscillator under seismic load is:

$$m \ddot{x}_S + 2 \beta_{air} \omega_{air} m \dot{x}_S + k x_S = -m \ddot{x}_0 \quad (1)$$

where x_0 is the seismic displacement, and x_S the relative displacement of the oscillator: $x_S = x_{S\,abs} - x_0$, where $x_{S\,abs}$ is the absolute displacement of the oscillator. The reduced damping β_{air} corresponds to the structural damping of the structure.

3.2 In-air row model

The dynamic equation of a 6-assembly row uses vectorial notations:

$$M \ddot{X}_S + K X_S = -M U \ddot{x}_0 \quad (2)$$

where X_S is the vector of the relative displacements of the assemblies of the row. M is a diagonal matrix (value m for the diagonal terms). K is a diagonal matrix also, with the value k . U is the vector (1; 1; 1; 1; 1; 1); \ddot{x}_0 , the seismic acceleration, is a scalar value. The only interactions between the oscillators are impacts, with a value of $2.4 \cdot 10^8$ N/m for the impact stiffness. This value is taken from previous two-beam model studies. The equations corresponding to this model can be solved using a modal basis, in a numerical code, with external forces for the impacts when they occur. For a 6-assembly row, the modal basis obviously comprises 6 modes which have the same frequency: $f = f_{air}$. Any displacement vector ($x_1 \ x_2 \ x_3 \ x_4 \ x_5 \ x_6$) can be a modal vector, in so far as the orthogonality properties of the modal basis are fulfilled.

3.3 Inertial effects of the fluid

The study of hydrodynamic coupling is commonly based on two assumptions. First, the fluid is a perfect fluid, with two equations to describe its behaviour: $\rho \frac{d\vec{V}}{dt} = -\vec{\nabla} P$ and $div \vec{V} = 0$. Second, the displacements of the structures are much smaller than the dimensions of the structures. As PWR fuel assemblies are regular fuel rods arrays, arranged in a regular pattern, many studies have been performed with the objective of homogenizing the dynamic behaviour of such structures (Brochard and Hammami [3], Cheval [4]). We will use the main results of these studies to build a model for the fluid structure interaction in the dynamic behaviour of a fuel assembly row.

In the study of a fuel assembly row, with confining lateral structures, it is possible, for symmetry reasons, to consider only one row of rods, instead of the 17 x 17 array. Brochard and Hammami [3] based their analysis on the study of an elementary cell, corresponding to one fuel rod (Figure 4). For slight differences in the accelerations of two adjacent rods, the force applied to the rod by the fluid is:

$$F_R = - m_{AR} \ddot{x}_{R abs} + (m_{AR} + m_{DR}) \ddot{x}_{L abs} \quad (3)$$

where F_R is the applied force, m_{AR} is the added mass for the rod, and m_{DR} the mass of fluid displaced by the rod. $x_{R abs}$ is the rod displacement, $x_{L abs}$ is the mean fluid displacement through the cell, both absolute. We can call the fluid acceleration "Darcy's acceleration", by analogy with the "Darcy's velocity" used in hydrology or for fluid flow in porous media. (De Marsily [5]). It is noteworthy that, with this expression, the applied force for $\ddot{x}_{R abs} = \ddot{x}_{L abs} = \ddot{x}$ is the "Archimede" force: $F = m_{DR} \ddot{x}$.

For a bundle of rods, from a theoretical point of view, this approach is valid only for identical accelerations of the rods. It is no longer valid when there are differences in the accelerations. Cheval [4] points out that, for a space periodic acceleration, with a space period of n rods, the error is large for the low values of n , with a maximum for opposite movements for adjacent rods ($n = 2$, space period of 2 rods). This approach can obviously be used in our case, as in an assembly the 17 rods have the same acceleration. The error at the boundaries between two assemblies, where adjacent rods may have different accelerations, is qualitatively the same as the error for a row of rods and a space period of 34 rods, and is small. This expression of the force applied by the fluid will be used in the case of an assembly row, immersed in a vessel, with lateral confinement structures (Figure 3). For the assembly number i :

$$F_i = - m_A \ddot{x}_{Si} + (m_A + m_D) \ddot{x}_{L abs} \quad (4)$$

where m_A and m_D correspond to the assembly. x_{Si} is the absolute displacement of the assembly i . For the assembly row, introducing the relative displacements, we obtain:

$$F = - M_A \ddot{X}_S + M_D U \ddot{x}_0 + (M_A + M_D) U \ddot{x}_L \quad (5)$$

F is the vector of the forces, \ddot{X}_S and U are the vectors defined for the in air row model (§ 3.2), and x_L is the relative displacement of the fluid ($x_L = x_{L abs} - x_0$ is a scalar value). This is a general expression, and for both configurations of the 6-assembly row (full confinement and lateral confinement), the fluid relative acceleration \ddot{x}_L will be expressed as a function of the absolute acceleration \ddot{x}_0 and of the row acceleration \ddot{X}_S . The elimination of \ddot{x}_L will then permit the dynamic equation of the rod to be determined, for both cases.

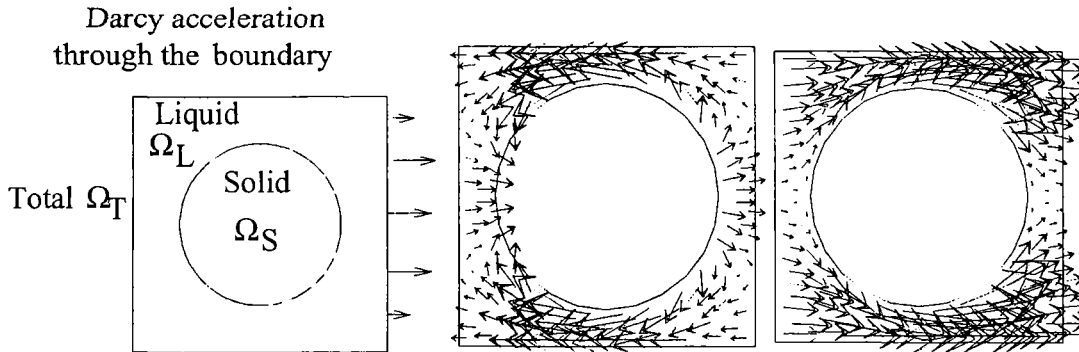


Figure 4: Elementary cell, fluid accelerations for rod motion, and for fluid motion

3.4 Dissipative effects

Water is commonly considered as a perfect fluid in vibration problems, which lead to negligible friction effects, as the displacements of the structure are small with respect to the structure dimension. In our case, the hypothesis of small displacements is no longer valid, since the displacement of a 1 cm diameter rod is a few centimeters. Fluid flow will take place through the assembly, where dissipative effects can be estimated approximately with the stationary flow hypothesis. The velocity of an assembly section can reach values of 0.5 m/s. If no overall motion movement is allowed for the fluid, local fluid motions will take place, with a maximum velocity of about $V_L = -1.5$ m/s. The relative velocity will be about $V = 2$ m/s (Figure 5). With a characteristic length L equal to the rod diameter, and with $\nu = 10^{-6}$ for the kinematic viscosity of water at ambient temperature, the Reynolds number will be: $Re = 18\ 000$. Many expressions give the force applied by the fluid on a solid, or the fluid head loss in different configurations (Schlichting [6]). The force applied on a cylinder (representing a single rod) in a stationary flow is: $F \simeq -\frac{1}{2}\rho_L S V^2$ where S is the section of the cylinder in the direction of the flow. Due to the proximity of the others rods, it seems preferable to use the expression of the head loss due to the sudden expansion of the flow channel, in the space between two rods (Figure 5): $\Delta P = \frac{1}{2}\rho_L(V - v)^2$ where V and v are the maximum and minimum velocities of the fluid. With $v \simeq 0.3 V$, we obtain $\Delta P = \frac{1}{4}\rho_L V^2$ and an applied force on the rod: $F = -\frac{1}{4}\rho_L S V^2$. With the notations D for the rod diameter, and H for the height, the dissipative force per rod is: $F = -\frac{1}{4}\rho_L D H V^2$

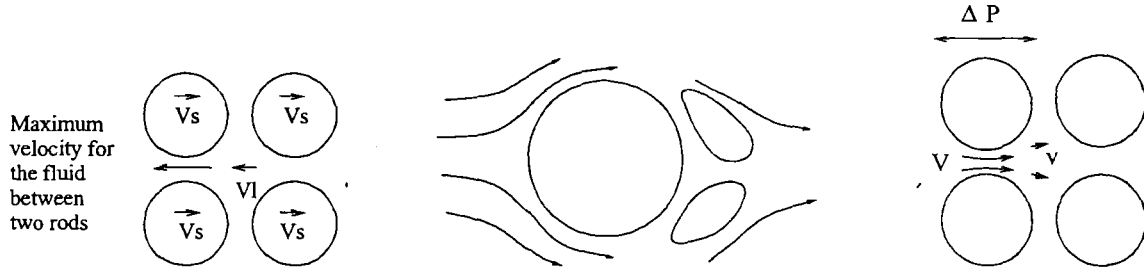


Figure 5: Relative fluid and solid velocities for dissipative effects

We consider now the dynamic equation of the assembly for a sine motion at the first and predominant natural frequency, with an amplitude A . From the velocity amplitude ωA and the acceleration amplitude $\omega^2 A$, it is easily derived that the amplitude of the inertial force is $F_i = M \omega^2 A$, and that of the dissipative force is: $F_d = 2 \beta M \omega^2 A$ (M is the assembly mass). The reduced damping is then $\beta = \frac{1}{2} \frac{F_d}{F_i}$.

As both F_i and F_d are proportional to the number of rods, they can be considered per rod for the estimation of β . The inertial force is $F_i = \pi/4 \rho_S D^2 H \omega^2 A$, where ρ_S is the average density of the rod. As the amplitude of the relative velocity of the fluid is $4\omega A$ from previous considerations, the dissipative force is $F_d = \frac{1}{4} \rho_L D H \omega^2 (4A)^2$. We finally obtain $\beta = \frac{1}{2} \frac{F_d}{F_i} \simeq \frac{8 \rho_L A}{\pi \rho_S D}$. For $A = 1.2 D$ (displacement 12 mm and diameter 10 mm) and $\rho_L/\rho_S = 0.1$, we get: $\beta = 0.3$.

The value of 30% is only a rough estimation, but which indicates clearly that dissipative effects can be very high in assembly seismic tests in water even without axial flow. The damping value depends on the fluid relative velocity. The value of 30% corresponds to a full confinement configuration, and for a lateral confinement configuration the value will be lower. The first interpretations of the snap back tests and sine sweep tests, performed on one assembly, give the following values for the damping in three configurations; in air: $\beta \simeq 10\%$, lateral confinement: $\beta \simeq 20\%$, full confinement: $\beta \simeq 30\%$ (Queval [2]).

3.5 Row model with full confinement configuration

The relative acceleration \ddot{x}_L of the fluid is equal to zero (the absolute acceleration of the fluid $\ddot{x}_{L\ abs}$ is equal to the acceleration of the tank \ddot{x}_0). The fluid force vector (§3.3) becomes (equation (5) with $\ddot{x}_L = 0$):

$$F = -M_A \ddot{X}_S + M_D U \ddot{x}_0 \quad (6)$$

If we add this force to the right hand side of equation (2) (dynamic equation in air, §3.1), in order to take into account the inertial effects of the fluid, we obtain the following dynamic equation:

$$(M + M_A) \ddot{X}_S + k X_S = -(M - M_D) U \ddot{x}_0 \quad (7)$$

M_A is a diagonal matrix: there are no interactions between the assemblies. As for the in air row model, the 6 assemblies are independent, and have the same natural frequency, corresponding to full confinement $f = f_{air} \sqrt{\frac{m}{m + m_A}}$. Therefore a value $\beta = 30\%$ is taken for the 6 modes.

3.6 Row model with lateral confinement configuration

In the lateral confinement configuration, a fluid relative acceleration takes place. This acceleration \ddot{x}_L is due to the relative acceleration of the assemblies, and is proportional to the sum of these accelerations. This relation can be expressed, using scalar values: $(m_A + m_D) \ddot{x}_L = m_C \sum_6 (\ddot{x}_{S_i} - \ddot{x}_0)$ where m_C is the coupling mass between the assemblies. Calculations performed for lateral confinement conditions (Figure 6) lead to the value $m_C = 1/12 m_A$.

In order to be used in the dynamic equation, this relation can also be expressed by using a full matrix M_C , with all terms equal to m_C : $(M_A + M_D) \ddot{x}_L U = M_C \ddot{X}_S$, where the vectors \ddot{X}_S and U , the matrix M_A and M_D have been presented in §3.2. The dynamic equation in the lateral confinement configuration is then:

$$(M + M_A - M_C) \ddot{X}_S + k X_S = -(M - M_D) U \ddot{x}_0 \quad (8)$$

As M_C is not a diagonal matrix, interactions between the assemblies will take place. The added mass matrix $M_A - M_C$ contains $m_A - m_C$ for the diagonal terms, and $-m_C$ for the other terms.

With these coupling feature, two groups of modes are obtained for the row, with two distinct frequencies. The first five modes (vectors V_1 to V_5) which correspond to no overall fluid motion since the sum of the assembly displacements is zero, have the same frequency as with full confinement, i.e. $f = f_{air} \sqrt{\frac{m}{m + m_A}}$ (§ 3.5).

$$\begin{aligned} V_1 &= 1 - 1 \ 0 \ 0 \ 0 \ 0 \\ V_2 &= 0 \ 0 \ 1 - 1 \ 0 \ 0 \\ V_3 &= 0 \ 0 \ 0 \ 0 \ 1 - 1 \\ V_4 &= 1 \ 1 \ 0 \ 0 - 1 - 1 \\ V_5 &= 1 \ 1 - 2 - 2 \ 1 \ 1 \\ V_6 &= 1 \ 1 \ 1 \ 1 \ 1 \ 1 \end{aligned}$$

The sixth mode (vector V_6), which corresponds to an identical motion of all assemblies and therefore implies an overall fluid motion, has a frequency $f' = f_{air} \sqrt{\frac{m}{m + m'_A}}$. The value of the equivalent added mass at assembly m'_A corresponds to the sum of all the coupling terms for the assembly because of the row rigid body motion, i.e.: $m'_A = (m_A - m_C) - 5m_C = m_A - 6/12m_A = m_A/2$.

From the previous modal properties, the modal damping values are logically set at $\beta = 30\%$ for modes 1 to 5, and $\beta = 20\%$ for mode 6.

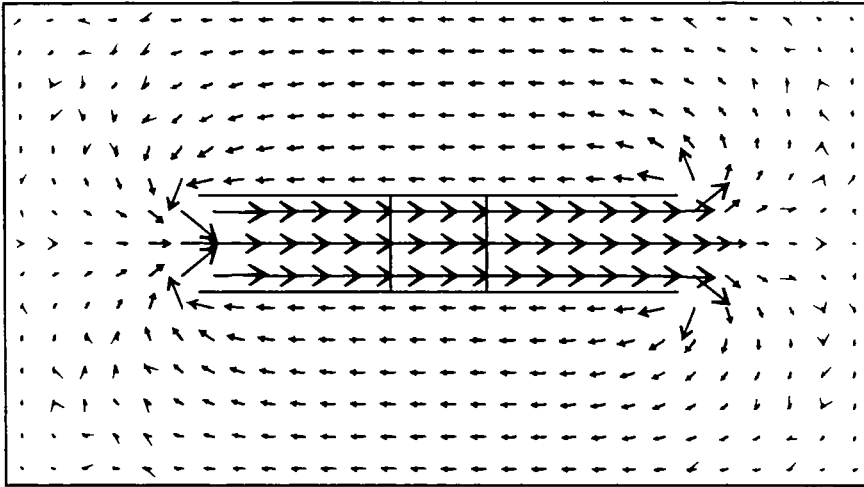


Figure 6: Low confinement fluid flow

4 Results of the theoretical model

The main results of the theoretical row model are presented in figures 8 to 10: For each of the 7 impact positions (0, 1, 2, 3, 4, 5, and 6), the figures give the value of the maximum impact force. Each figure includes 30 curves, as 30 different accelerograms were used in the seismic tests, corresponding to the same response spectrum (only 15 accelerograms for the full confinement) (Figure 7). Figure 8 gives the results for the tests in air, Figures 9 and 10 display the results for the tests in the lateral and full confinement configurations. These results exhibit two main features: the scatter range due to the load signal is about 30%, and the maximum impact forces are higher for the in air simulations and, in water, lower for the complete confinement configuration. These results from calculations correspond qualitatively to the experimental ones.

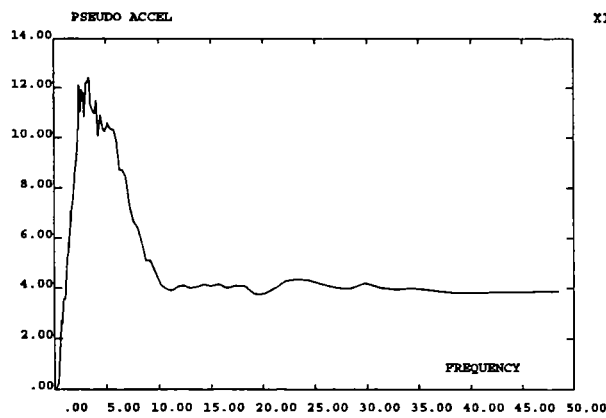


Figure 7: Response spectrum

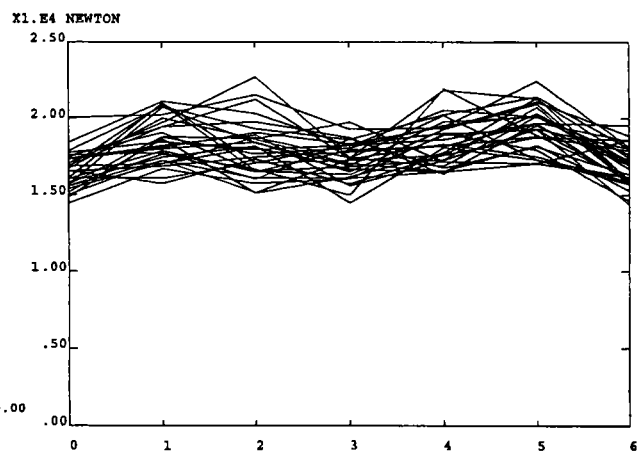


Figure 8: Maximal Forces in air

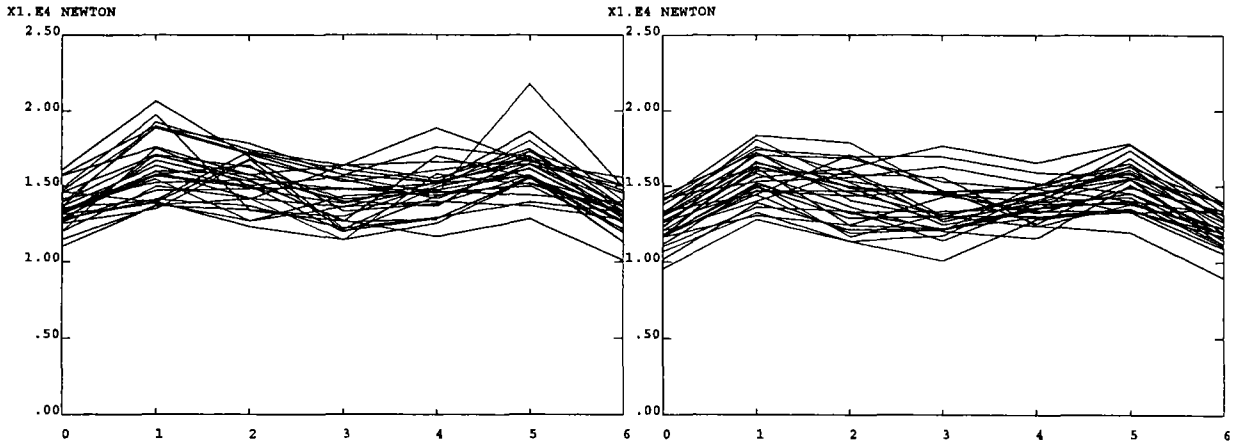


Figure 9: Maximal Forces for lateral confinement

Figure 10: Maximal Forces for full confinement

Conclusion

A model of the assembly row which has undergone the seismic tests was built, based on a single DOF assembly model representing the first predominant mode, but with a complete hydrodynamic coupling model, and damping due to the fluid motion. For both inertial and dissipative effects, the fluid structure interaction models are based on simple physical considerations about the structural and fluid motions, related by continuity. It is shown that frequencies and damping are primarily influenced by the existence of an overall fluid motion along the row, which is not possible with the full confinement, and depends on the out-of-phase or in-phase character of the assembly displacements in the modes of the row with the lateral confinement. Calculations of the impact forces during the seismic tests were performed; the calculation and test results prove consistent with respect to the influence of the test conditions, since they exhibit very similar decrease of the impact forces in water, enhanced with full confinement, mainly because of the larger damping. Further studies are under way on assembly row models with beam models for the assemblies; but the simplified assembly model used in the present work can also prove efficient for analysing the fluid coupling effects in core models including several rows, for a better estimation of the validity of the standard model.

References

- [1] J. Rigaudeau. Hydrodynamic Coupling in Seismic Response of PWR Fuel Assemblies and Other Immersed Structures. ASME PVP, Vol 394, 201-208, Boston 1999.
- [2] JC Queval. Seismic Tests of Interacting Full Scale Fuel Assemblies on Shaking Table. SMIRT 16, Washington 2001
- [3] D Brochard, I. Hammami. Non-Linear Analysis of Nuclear Reactor Cores by an Homogenization Method. ASME PVP, Vol 223, San Diego.
- [4] K. Cheval. Modélisation du Comportement Sismique de Structures Multitubulaires Baignées par un Fluide Dense. Thesis Evry 2001.
- [5] G. de Marsily. Hydrogéologie quantitative. Masson 1981.
- [6] H Schlichting, K Gersten. Boundary Layer Theory. Springer Verlag.
- [7] P Verpeaux, A Millard, T Charras, A Combesure. A Modern Approach of Computer Codes for Structural Analysis. SMIRT 10, Anaheim, 1989.

